ALGORITHM THEORETICAL BASIS DOCUMENT (ATBD):

TOTAL BIOMASS

PREPARED BY	ORGANIZATION	DATE
Bridget Hass	AOP	05/29/2019
Tristan Goulden	AOP	05/29/2019

APPROVALS	ORGANIZATION	APPROVAL DATE
David Barlow	SYS	06/11/2019

RELEASED BY	ORGANIZATION	RELEASE DATE
Anne Balsley	CM	07/01/2019

See configuration management system for approval history.

The National Ecological Observatory Network is a project solely funded by the National Science Foundation and managed under cooperative agreement by Battelle. Any opinions, findings, and conclusions or recommendations expressed in this material are those of the author(s) and do not necessarily reflect the views of the National Science Foundation.

CHANGE RECORD

REVISION	DATE	ECO #	DESCRIPTION OF CHANGE
A	07/01/2019	ECO-06170	Initial Release

TABLE OF CONTENTS

1 DESCRIPTION ... 3
1.1 Purpose ... 3
1.2 Scope ... 3
2 RELATED DOCUMENTS, ACRONYMS AND VARIABLE NOMENCLATURE ... 4
2.1 Applicable Documents ... 4
2.2 Reference Documents ... 4
2.3 Acronyms ... 4
3 DATA PRODUCT DESCRIPTION ... 5
3.1 Variables Reported ... 5
3.2 Input Dependencies ... 5
3.3 Product Instances ... 5
3.4 Temporal Resolution and Extent ... 5
3.5 Spatial Resolution and Extent ... 6
4 SCIENTIFIC CONTEXT ... 6
4.1 Theory of Measurement / Observation ... 6
4.2 Theory of Algorithm ... 7
4.3 Special Considerations ... 8
5 ALGORITHM IMPLEMENTATION ... 9
6 UNCERTAINTY ... 10
7 VALIDATION AND VERIFICATION ... 12
8 FUTURE PLANS AND MODIFICATIONS ... 13
9 BIBLIOGRAPHY ... 13

LIST OF TABLES AND FIGURES

Table 1 - Data products generated by algorithms described within this ATBD ... 5
Table 2 - Regression coefficients for NDVI-Biomass equation reported by Dong et al. (2003) ... 8

Figure 1 - Biomass as a function of latitude and NDVI ... 8

Figure 2 - Workflow for creating the biomass product 10

1 DESCRIPTION

1.1 Purpose

This document details the algorithms used for creating the NEON Level 2 Biomass data product (NEON.DOM.SITE.DP2.30016) from Level 1 data, and ancillary data (such as calibration data), obtained via instrumental measurements made by the Neon Imaging Spectrometer (NIS) sensor on the Airborne Observation Platform (AOP). It includes a detailed discussion of measurement theory and implementation, appropriate theoretical background, data product provenance, quality assurance and control methods used, approximations and/or assumptions made, and a detailed exposition of uncertainty resulting in a cumulative reported uncertainty for this product.

1.2 Scope

This document describes the theoretical background and entire algorithmic process for creating NEON.DOM.SITE.DP2.30016 from input data. It does not provide computational implementation details, except for cases where these stem directly from algorithmic choices explained here.

2 RELATED DOCUMENTS, ACRONYMS AND VARIABLE NOMENCLATURE

2.1 Applicable Documents

AD[01]	NEON.DOC.000001	NEON Observatory Design (NOD) Requirements
AD[02]	NEON.DOC.002652	NEON Level 1, Level 2 and Level 3 Data Products Catalog
AD[03]	NEON.DOC.002293	NEON Discrete LiDAR datum reconciliation report
AD[04]	NEON.DOC.002649	NEON configured site list

2.2 Reference Documents

RD[01]	NEON.DOC.000008	NEON Acronym List
RD[02]	NEON.DOC.000243	NEON Glossary of Terms
RD[03]	NEON.DOC.005011	NEON Coordinate Systems Specification
RD[04]	NEON.DOC.002890	NEON AOP Level 0 quality checks
RD[05]	NEON.DOC.001984	AOP flight plan boundaries design
RD[06]	NEON.DOC.001292	NEON Imaging Spectrometer Geolocation Algorithm Theoretical Basis Document
RD[07]	NEON.DOC.001288	NEON Imaging Spectrometer Radiance to Reflectance Algorithm Theoretical Basis Document
RD[08]	NEON.DOC.002391	NEON Normalized Difference Vegetation Index (NDVI), Enhanced Vegetation Index (EVI), Atmospherically Resistant Vegetation Index (ARVI), Canopy Xanthophyll Cycle (PRI), and Canopy Lignin (NDLI) Algorithm Theoretical Basis Document

2.3 Acronyms

Acronym	Explanation
AGB	Above Ground Biomass
NIS	NEON Imaging Spectrometer
ITRF00	International Terrestrial Reference Frame 2000
UTM	Universal Transverse Mercator
TIFF	Tagged Image File Format
AGB	Above Ground Biomass
AOP	Airborne Observation Platform
FBO	Fixed Base Operator
NDVI	Normalized Difference Vegetation Index
VI	Vegetation Index
ASPRS	American Society of Photogrammetry and Remote Sensing

3 DATA PRODUCT DESCRIPTION

3.1 Variables Reported

The products supplied through NEON.DOM.SITE.DP2.30016 include a biomass map, in raster format by flight line. The biomass maps are derived from the directional surface reflectance RD[07], through the intermediate NDVI (Normalized Difference Vegetation Index) product. Biomass maps are reported with horizontal reference to the ITRF00 datum, projected to the Universal Transverse Mercator (UTM) mapping frame in accordance with RD[03]. The biomass is reported as g/m^2 value which describes the total weight of vegetative material. The product is stored in a GeoTIFF format in accordance with the GeoTIFF specification (Ritter et al., 2000).

3.2 Input Dependencies

The creation of biomass rasters is dependent on the creation of the bi-directional surface reflectance, and is based on the NDVI products. Procedures for creating NDVI can be found in RD[08].

3.3 Product Instances

The NEON data products produced directly from these algorithms are summarized in Table 1.

Table 1 - Data products generated by algorithms described within this ATBD

Data product identification	Data product name
NEON.DOM.SITE.DP2.30016	Biomass

3.4 Temporal Resolution and Extent

The biomass product is derived from data collected during acquisition of a single core, re-locatable or aquatic site by the AOP (Airborne Observation Platform). Depending on external variables such as weather, transit time to the site FBO (Fixed Based Operator), and total area of the priority 1 flight box (see RD[05]), the temporal resolution of a single acquisition of L0 NIS information could range from a single flight (4 hrs.) to several flights acquired over multiple days. Generally, due to the peak greenness constraint of AOP data acquisition (site at > 90% peak greenness value), and the requirement that all sites are to be flown annually, the total potential time to acquire a site will have a limit which defines the largest temporal resolution for a single acquisition. Details defining the total amount of potential time dedicated to a single site acquisition are given in RD[05]. As the NEON AOP payload is scheduled to repeat each NEON site on an annual basis, the temporal resolution of multiple acquisitions will be one year.

3.5 Spatial Resolution and Extent

The spatial resolution and extent of the biomass product will be equivalent to the spatial resolution and extent of the surface directional reflectance. The biomass product relies on the intermediate calculation of NDVI (RD[08]), which shall maintain 1 m spatial resolution. The spatial extent of the biomass maps will relate to the definition of the AOP flight box for each individual site (RD[04]). It is intended that a minimum of 80% of the priority 1 flight box and 95% of the tower airshed will be acquired each year (RD[07]). As discussed in Section 3.4, the actual acquired area could vary depending on external conditions encountered during the flight. Ultimately, the flight schedule as defined in RD[04] shall supersede the percent coverage requirement. Therefore, the actual acquired spatial extent may vary annually.

4 SCIENTIFIC CONTEXT

The world's forest ecosystems are a critical variable in quantifying changes in annual global carbon budgets due to their carbon storage potential. Accurate quantification of potential annual uptake and storage of carbon by forests is critical for long term forecasting of greenhouse gas emissions due to their offsetting effect. Aboveground biomass density (AGB) is a biophysical quantity that can be used as a proxy for carbon content and sequestration. As such, AGB is a primary input for models of the terrestrial carbon budget, which is known to be the least constrained component of the global budget (Bloom, Exbrayat, van der Velde, Feng, & Williams, 2016),(Le Toan et al., 2011) (Houghton, Hall, & Goetz, 2009), (Schimel, House, Hibbard, Bousquet, et al., 2001). Developing estimations of spatial and temporal patterns of biomass is also useful for monitoring the ecosystem impacts of natural and anthropogenic events, such as forest fires, drought, deforestation, urbanization, and land-use changes (Koch, 2010), (Lu et al., 2012). Quantifications of AGB can help inform policy decisions pertaining to agricultural and wildfire management, sustainable forestry practices, bio-energy resources, and carbon sequestration (Man, Dong, Guo, Liu, & Shi, 2014).

4.1 Theory of Measurement / Observation

Optical satellite remote sensing data has become a primary source for continental and global scale biomass estimation, largely due to the extensive spatial coverage and availability of Landsat data (Lu et al. (2016),Man et al. (2014), Goetz et al. (2009)). A number of studies have related spectral variables (e.g. vegetation indices, textural measures, etc.) to field measurements of biomass, using either multiple regression analysis or non-parametric methods. Spectral indexes are often exploited for biomass estimation because they relate to the relative amount of reflected solar energy in photosynthetically active wavelengths in vegetation, allowing inference on the overall photosynthetic capacity. It follows that there will be a positive correlation between photosynthetic capacity and biomass. Most studies estimating biomass from hyperspectral data focus on a small case-study area featuring a unique ecosystem type (e.g. Cho, Skidmore, Corsi, Van Wieren, and Sobhan (2007), Goswami, Gamon, Vargas, and Tweedie (2015)), while studies encompassing larger spatial extents typically implement multiple data sources ((Hu et al., 2016),(Su et al., 2016),(Saatchi et al., 2011)). Estimations of biomass from single-sensor data have restrictive limitations, discussed in section 4.3 and 7, but can still provide a baseline estimate. Several ecological studies have developed relationships relating NDVI to biomass, despite a known saturation of NDVI at high biomass values. The NDVI-biomass equation published by Dong et al. (2003) was selected to produce a preliminary biomass product because it is the most comprehensive analysis relating biomass to NDVI for forests in the continental U.S.

4.2 Theory of Algorithm

Biomass is calculated according to functional biomass relationship with NDVI and latitude, as reported by Dong et al. (2003):

$$\frac{1}{Biomass} = \alpha + \beta\left[\frac{\frac{1}{NDVI}}{Latitude^2}\right] + \gamma Latitude$$

where α, β, and γ are regression coefficients summarized in **Table 2**. The coefficients were estimated using ordinary least squares regression comparing the cumulative growing season NDVI to National Forest Resource Inventory data of six industrialized temperate -boreal countries (Canada, Finland, Norway, Russia, Sweden, and USA). The global 8 x 8 km resolution NDVI dataset was derived from Advanced Very High Resolution Radiometers (AVHRR) on board the NOAA-7,-9, -11, and -14 satellites run by the Global Inventory Monitoring and Modeling System (GIMMS) group (Los, Justice, & Tucker, 1994). Inventory data for the USA was obtained from the USDA Forest Inventory and Analysis database, downloadable from https://www.fia.fs.fed.us/tools-data/. The relationship depends only on the latitude of the site as well as the NDVI of the vegetation (**Figure 1**).

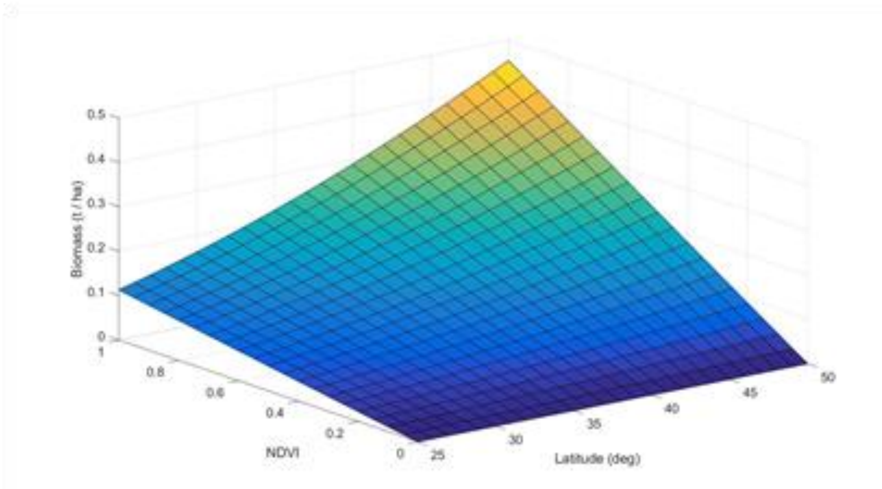

Figure 1 - Biomass as a function of latitude and NDVI

Table 2 - Regression coefficients for NDVI-Biomass equation reported by Dong et al. (2003)

Variable	Value	Standard Error
Α	-0.0557	0.0136
Β	5548.05	1274.17
Γ	0.000854	0.000153

4.3 Special Considerations

There are known critical limitations in using solely hyperspectral data, and more generally any single-sensor data, for approximating biomass; 1) Hyperspectral data contains useful information about the spectral reflectance at the top- of-canopy, but not the three dimensional structure (i.e. density) below canopy and the understory, which are essential parameters for biomass estimation, 2) spectral indices derived from optical sensor data are subject to saturation at sites with high biomass density, which affects the upper limit of biomass estimation. Biomass calculated from the Dong et al. (2003) NDVI-biomass equation saturates at 180 g/m2 at the highest latitudes in the continental US, and at 60 g/m2 at the lowest latitudes Figure 1, 3) modeled relationships can be sensor, scale and site specific. For example, Dong et al. (2003) acknowledge that their equation poorly approximates biomass in certain ”US temperate forests, where biomass is either uncharacteristically low (southern states) or high (pacific northwest states)”. Because spectral indices, in this case NDVI, are reflectance band ratios, they can be unstable if not used in the correct setting (e.g. non-vegetated areas), which carries over into the biomass product.

Biomass can be calculated with higher accuracy if the structural information from the laser scanner and spectral information from the imaging spectrometer are used in synergy, along with field measured tree parameters (i.e. diameter at breast height, tree height, crown width) to develop allometric relationships to appropriately train modeled estimates. At the time of writing, neither a standardized and accepted algorithm for calculating AGB was available, or appropriate tree measurements for developing allometric equations across the NEON sites. Future availability of these measurements will allow further development and testing of the algorithm as the community develops standardized approaches for calculation of biomass from remote sensing data. Nevertheless, the Dong et al. (2003) relationship is applied here as the best available estimate, despite its limitations. Further information on the data product uncertainty can be found in Section 6.

5 ALGORITHM IMPLEMENTATION

The processing of surface reflectance into the biomass product is achieved through the steps outlined in this section (Figure 2). The algorithm for Biomass is implemented through multiple interconnected Matlab functions which automate the algorithm. The process is dependent on only the existence of a Normalized Difference Vegetation Index (NDVI) geotiff and the model parameter inputs. Details into the algorithm which creates the NDVI from input surface reflectance can be found in RD[08].

Step 1:
Calculate NDVI from surface reflectance according to RD[08].

Input:

1. reflectance data (HDF5 format)

Output: NDVI in geotiff format

Functions used: NEONAOPVegIndexer.pro

Step 2:
Calculate biomass raster according to Equation (1) using output from Step 1.

Input:

1. NDVI from Step 1

Output: Biomass in geotiff format

Functions used: calc_spec_biomass_v01.m

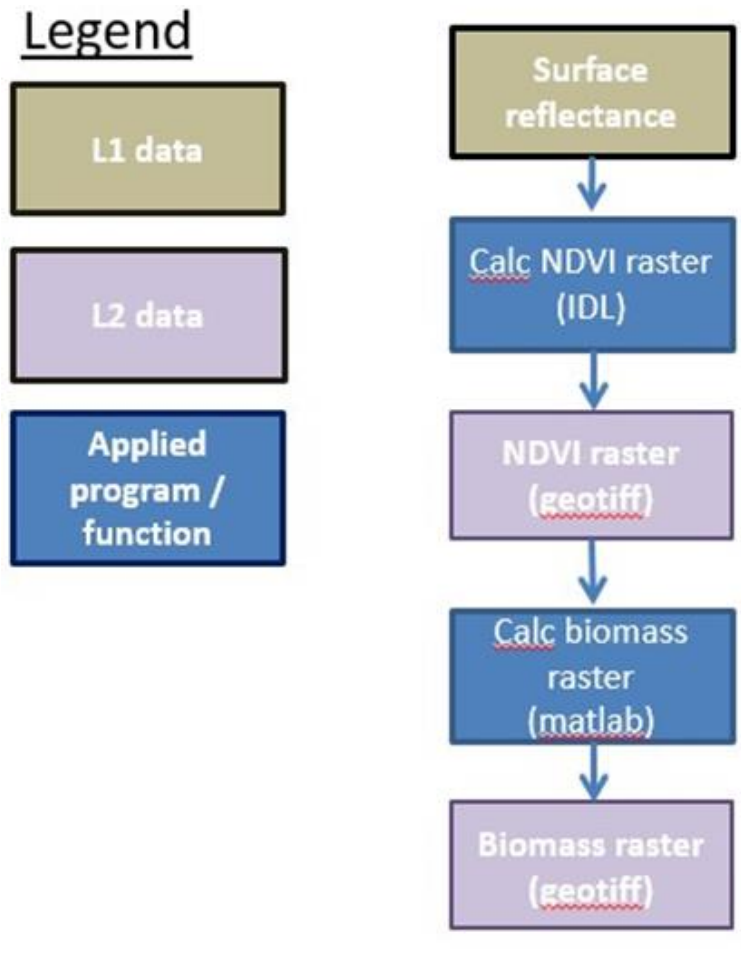

Figure 2 - Workflow for creating the biomass product

6 UNCERTAINTY

The uncertainty in the biomass is derived from several sources of error including;

1. calibration of the sensor
2. quality of geometric co-registration of the spectral bands
3. quality of the ortho-rectification
4. accuracy of the radiative transfer code (MODTRAN 5)
5. correct choice of the atmospheric input parameters
6. terrain type (flat vs. rugged)
7. surface cover

NEON undertakes annual calibrations of the imaging spectrometer, which will minimize errors due to source 1. Currently, the uncertainty introduced through calibration is not strictly quantified and propagated into derived products. Vicarious calibration surveys are performed over homogeneous targets (concrete, consistent low vegetation) at the beginning and end of the annual flight campaign, including ground validation of targets with known reflectance measured with a field spectrometer. This information allows an annual empirical assessment of the calibration uncertainty which is used to verify the quality of the calibration. Additional research will be necessary to propagate the calibration uncertainty through to final products. Results of the annual vicarious calibration tests indicate that the error is small (<0.5%), indicating its effect may be negligible.

Internal testing has shown sub-pixel accuracy of the ortho-rectification (source 3), which is based on a spectrometer camera model described in RD[06]. The individual spectral bands are collected simultaneously on a single focal plane array, introducing negligible error in co-registration between spectral bands (source 2). Therefore, it can be assumed that the geo-location error does not introduce a significant level of uncertainty into resulting surface reflectance in flat or smoothly undulating terrain. However, as identified in richter2012atmospheric highly rugged terrain such as mountainous environments can introduce a mis-registration between the DSM and reflectance measurements, which can cause errors in surface reflectance greater than ±100% (due to error source 6). Richter (2012) atmospheric recommend that the DSM spatial resolution is one-third or one-quarter the spatial resolution of the imaging spectrometer data. However, the DSMs at NEON are created at equivalent resolutions (1 m) due to limitations in the point density of the LiDAR system. At current nominal altitudes and LiDAR system collection parameters, the resulting point spacing is not capable of confidently supporting DSM grid resolutions below 1 m spatial resolution. Therefore, users should be aware that data located near sharp peaks or ridges should be treated with extreme caution, as the uncertainty may be extremely high. NEON data does maintain an advantage in reducing uncertainty due to terrain effects by simultaneously collecting the NIS and LiDAR from co-mounted sensors on the same platform, and creating the spectrometer camera model using intensity images from the LiDAR. This provides a high level of relative accuracy between the DSM and spectrometer, minimizing uncertainty due to the terrain conditions. Typically, geo-location errors are highest at strip edges due to limitations in derivation of the geo-location model (see RD[06]). Therefore, the combination of mountainous terrain and data acquired at strip edges will introduce the largest sources of uncertainty in geo-location.

The retrieval of surface reflectance is performed with ATCOR, which is a commercial off-the-shelf software package (see RD[07]), preventing NEON from controlling the uncertainty introduced through source 4, the accuracy of radiative transfer code derived from MODTRAN 5. It is assumed that this is being correctly implemented within ATCOR, and that efforts to minimize the uncertainty due to this source were applied. User's should be aware that ATCOR does not explicitly calculate a radiative transfer model for every observation. For processing efficiency, ATCOR pre-generates a series of look-up tables which are representative of common atmospheric and flight conditions (altitude, aerosol loading, visibility humidity etc.). Some uncertainty will be introduced through interpolation of true conditions to the most representative scenarios in the look up tables (LUTs). Assuming error source 4 is well controlled within ATCOR and appropriate conditions are available in the LUTs, the primary source of error affected by NEON processing procedures is due to source 5, the correct choice of atmospheric input parameters. Currently, a standard set of parameters is selected across all NEON sites, and no attempt is made to dynamically vary the input parameters for unique site conditions. Details into the implemented input parameters can be found in RD[07]. As the NEON project continues, research will be undertaken to allow the conditions experienced during flight to inform the correct selection of parameters for atmospheric correction, and better quantify the uncertainty introduced in these choices.

The aforementioned sources of uncertainty each relate to errors introduced through the instrument or processing of reflectance data, however, the largest source of uncertainty in the biomass product is likely the empirical equation used to relate NDVI to biomass (see Equation (1)). This relationship may not be valid for spectral-biomass relationships of the alternative instruments, study areas, and spatial and temporal scales of the NEON airborne remote-sensing data, which have unique acquisition parameters, calibration, and processing procedures. The Dong et al. (2003) equation was developed using satellite remote sensing data with a pixel resolution of 8km x 8km, while NEON hyperspectral data is acquired with 1 m^2 resolution. Uncertainty introduced through the scaling a mesoscale relationship to fine-scale pixels at the individual scale, will undoubtedly result in unacceptable levels of uncertainty. For example, the relationship derived in Dong et al. (2003) included highly heterogeneous individual pixels, often compromising multiple forest and land use types. It is unlikely that forcing this relationship on fine-scale resolution imagery with nearly homogeneous individual pixels will be accurate, and the level of uncertainty will be difficult to quantify. The relationship may be valid under conditions of a nearly homogeneous landscape (Wu & Li, 2009), which is atypical for NEON study areas. As such, it is currently recommended that the biomass estimates are used with caution, as the absolute values are likely to be highly inaccurate. The biomass product in its current form would be best used only as a relativistic biomass comparison, not as an absolute estimate.

7 VALIDATION AND VERIFICATION

A number of biomass maps have been produced spanning the continental U.S., but there is still considerable variation and uncertainty in these reported values (Neeti and Kennedy, 2016, Hill, Williams, Bloom, Mitchard, and Ryan, 2013). Accurately estimating continental biomass is still an active research topic. Given the variability of reported biomass values, validation for this data product was carried out by 1) comparing results with existing biomass models to see if it lies within the range of published values, and 2) comparing the NDVI-derived biomass with biomass estimated from LiDAR data for a single site as a test case.

8 FUTURE PLANS AND MODIFICATIONS

Further research is required in order to develop a more robust estimate of biomass from NEON hyperspectral data. Lu et al. (2016) outline a more comprehensive procedure for modeling biomass from remote-sensing data, which includes “field survey data collection, biomass calculation at plot level, remote sensing data selection, variable extraction, proper algorithm selection, and error evaluation”. Future enhancements will be made to the biomass product, which include multi-sensor fusion and integration of appropriate allometric equations as calibration / validation data.

9 BIBLIOGRAPHY

Bloom, A. A., Exbrayat, J.-F., van der Velde, I. R., Feng, L., & Williams, M. (2016). The decadal state of the terrestrial carbon cycle: global retrievals of terrestrial carbon allocation, pools, and residence times. Proceedings of the National Academy of Sciences, 113(5), 1285–1290.

Cho, M. A., Skidmore, A., Corsi, F., Van Wieren, S. E., & Sobhan, I. (2007). Estimation of green grass/herb biomass from airborne hyperspectral imagery using spectral indices and partial least squares regression. International Journal of Applied Earth Observation and Geoinformation, 9(4), 414–424.

Dong, J., Kaufmann, R. K., Myneni, R. B., Tucker, C. J., Kauppi, P. E., Liski, J., … Hughes, M. K. (2003). Remote sensing estimates of boreal and temperate forest woody biomass: carbon pools, sources, and sinks. Remote Sensing of Environment, 84(3), 393–410.

Glenn, E. P., Huete, A. R., Nagler, P. L., & Nelson, S. G. (2008). Relationship between remotely-sensed vegetation indices, canopy attributes and plant physiological processes: what vegetation indices can and cannot tell us about the landscape. Sensors, 8(4), 2136–2160.

Goetz, S. J., Baccini, A., Laporte, N. T., Johns, T., Walker, W., Kellndorfer, J., … Sun, M. (2009). Mapping and monitoring carbon stocks with satellite observations: a comparison of methods. Carbon balance and management, 4(1), 2. Goswami, S., Gamon, J., Vargas, S., & Tweedie, C. (2015). Relationships of ndvi, biomass, and leaf area index (lai) for six key plant species in barrow, alaska. PeerJ PrePrints.

Hill, T. C., Williams, M., Bloom, A. A., Mitchard, E. T., & Ryan, C. M. (2013). Are inventory based and remotely sensed above-ground biomass estimates consistent? PLoS One, 8(9), e74170.

Houghton, R., Hall, F., & Goetz, S. J. (2009). Importance of biomass in the global carbon cycle. Journal of Geophysical Research: Biogeosciences, 114(G2).

Hu, T., Su, Y., Xue, B., Liu, J., Zhao, X., Fang, J., & Guo, Q. (2016). Mapping global forest aboveground biomass with spaceborne lidar, optical imagery, and forest inventory data. Remote Sensing, 8(7), 565.

Koch, B. (2010). Status and future of laser scanning, synthetic aperture radar and hyperspectral remote sensing data for forest biomass assessment. ISPRS Journal of Photogrammetry and Remote Sensing, 65(6), 581–590.

Le Toan, T., Quegan, S., Davidson, M., Balzter, H., Paillou, P., Papathanassiou, K., …, Shugart, H., et al. (2011). The biomass mission: mapping global forest biomass to better understand the terrestrial carbon cycle. Remote sensing of environment, 115(11), 2850–2860.

Los, S. O., Justice, C., & Tucker, C. (1994). A global 1 by 1 ndvi data set for climate studies derived from the gimms continental ndvi data. International Journal of Remote Sensing, 15(17), 3493–3518.

Lu, D., Chen, Q., Wang, G., Liu, L., Li, G., & Moran, E. (2016). A survey of remote sensing-based aboveground biomass estimation methods in forest ecosystems. International Journal of Digital Earth, 9(1), 63–105.

Lu, D., Chen, Q., Wang, G., Moran, E., Batistella, M., Zhang, M., … Saah, D. (2012). Aboveground forest biomass estimation with landsat and lidar data and uncertainty analysis of the estimates. *International Journal of Forestry Research*, *2012*.

Man, Q., Dong, P., Guo, H., Liu, G., & Shi, R. (2014). Light detection and ranging and hyperspectral data for estimation of forest biomass: a review. *Journal of Applied Remote Sensing*, *8*(1), 081598–081598.

Neeti, N. & Kennedy, R. (2016). Comparison of national level biomass maps for conterminous us: understanding pattern and causes of differences. *Carbon balance and management*, *11*(1), 19.

Saatchi, S. S., Harris, N. L., Brown, S., Lefsky, M., Mitchard, E. T., Salas, W., …, Hagen, S., et al. (2011). Benchmark map of forest carbon stocks in tropical regions across three continents. *Proceedings of the National Academy of Sciences*, *108*(24), 9899–9904.

Schimel, D. S., House, J. I., Hibbard, K. A., Bousquet, P., et al. (2001). Recent patterns and mechanisms of carbon exchange by terrestrial ecosystems. *Nature*, *414*(6860), 169.

Su, Y., Guo, Q., Xue, B., Hu, T., Alvarez, O., Tao, S., & Fang, J. (2016). Spatial distribution of forest aboveground biomass in china: estimation through combination of spaceborne lidar, optical imagery, and forest inventory data. *Remote Sensing of Environment*, *173*, 187–199.

Wu, H. & Li, Z.-L. (2009). Scale issues in remote sensing: a review on analysis, processing and modeling. *Sensors*, *9*(3),1768–1793.